Soft Matter

Accepted Manuscript


Volume 1 | Number 1 | Jan 2013 | Pages 1–100

Soft Matter

www.rsc.org/softmatter

ROYAL SOCIETY OF CHEMISTRY

ROYAL SOCIETY OF CHEMISTRY

www.rsc.org/softmatter

Journal Name

ARTICLE

Unexpected Role of Linker Position on Ammonium Gemini Surfactant Lyotropic Gyroid Phase Stability

Received 00th January 20xx,
Accepted 00th January 20xx

DOI: 10.1039/x0xx00000x

www.rsc.org/

Gregory P. Sorenson[a,†] and Mahesh K. Mahanthappa[a,b,*]

Arising from the water-driven self-assembly of amphiphiles over generally narrow temperature and composition phase windows, aqueous lyotropic liquid crystal (LLC) network phases are useful in applications as therapeutic delivery vehicles and templates for mesoporous material syntheses. While a clear set of amphiphile design rules that enables access to these intricate three-dimensional structures has yet to emerge, recent work indicates that bis(ammonium), bis(phosphonium), and dicarboxylate gemini ("twin tail") surfactants enable enhanced access to LLC network phases such as the double gyroid (G). In order to better understand the scope of this amphiphile design strategy, we investigated the synthesis and aqueous LLC self-assembly behaviors of a homologous series of quaternary gemini bis(ammonium) dichloride surfactants, in which we varied the position of the hydrophobic linker that connects the constituent single tail surfactants. These experiments demonstrate that the position of the linker directly impacts the maximum counterion-headgroup hydration capacity and the extent of counterion-headgroup association, all of which contribute to the aqueous lyotropic double gyroid network phase stability. Thus, judicious selection of the linker position in ionic gemini surfactants provides a new molecular design tool for manipulating LLC network phase stability.

Introduction

Small molecule amphiphiles self-assemble in concentrated aqueous media to form lyotropic liquid crystals (LLCs), as a consequence of thermodynamically preferential interactions between water and the hydrophilic surfactant headgroups.[1, 2] These non-covalent, supramolecular assemblies are characterized by their structurally periodic, nanoscale arrangements of hydrophilic and hydrophobic domains, in which the domain interfaces are decorated with the chemical functionality of the amphiphile headgroup. Phase selection in these systems depends primarily on the LLC composition, which is commonly reported as the surfactant weight fraction in H_2O, and on temperature to a lesser extent. LLCs are categorized as Type I structures if the hydrophobic domains are convex, whereas Type II structures exhibit concave hydrophobic domains. Well-known aqueous LLC morphologies include both Type I and Type II tetrahedrally- and hexagonally-closest packed point particle phases (I), hexagonally-packed cylindrical micelles (H), and bilayer or lamellar phases (L_α).[3, 4] In typically narrow LLC composition windows intermediate between the L_α and H phases, at least four triply periodic multiply continuous "network" phase LLCs have been observed: the double gyroid (G; $Ia\bar{3}d$ symmetry), double diamond (D; $Pn\bar{3}m$ symmetry), primitive (P; $Im\bar{3}m$ symmetry), and the recently reported tetracontinuous hexagonal network phase (H_I[193]; $P6_3/mcm$ symmetry),[5, 6] all of which exhibit hydrophilic/hydrophobic domain interfaces with negative Gauss ("saddle splay") curvature. Network phase LLCs are particularly useful as selective ion transporting materials,[7, 8] platforms for protein crystallization[9, 10], therapeutic nucleic acid delivery vehicles,[11, 12] and structure directing agents for mesoporous and nanoporous materials.[13-17] Thus, the development of new surfactant platforms that enable manipulation of both LLC structure and stability offer powerful "bottom up" methods for controlling the functionalities and physicochemical properties of these useful materials.

Recent studies of the LLC phase behaviors of gemini surfactants, derived from covalent dimerization of two single-tail surfactants at or near the hydrophilic headgroup, indicate their enhanced ability to stabilize technologically useful network phases (Figure 1a).[6, 8, 18-21] Gin and co-workers demonstrated that 4° bis(phosphonium)[20] and 4° bis(ammonium)[8] gemini surfactants exhibit aqueous lyotropic double gyroid (G_I) phases over amphiphile composition windows as wide as ~8–10 wt% between T = 22–80 °C. In and Zana further demonstrated that the extent of surfactant counterion-headgroup dissociation plays an important role in G_I–phase stability.[18] Complementary work by Alami *et al.* revealed that the length of the hydrophobic linker between the headgroups of a series of 4° bis(ammonium) gemini

---

[a] *Department of Chemistry, University of Wisconsin–Madison, 1101 University Ave., Madison, WI 53703.*
[b] *Department of Chemical Engineering & Materials Science, University of Minnesota, 421 Washington Ave., S.E., Minneapolis, MN 55455.*
† 3M Corporate Research Materials Laboratory 3M Center, St. Paul, MN 55144.

Electronic Supplementary Information (ESI) available: Detailed surfactant synthesis procedures, and representative SAXS data for coexisting LLC phases. See DOI: 10.1039/x0xx00000x

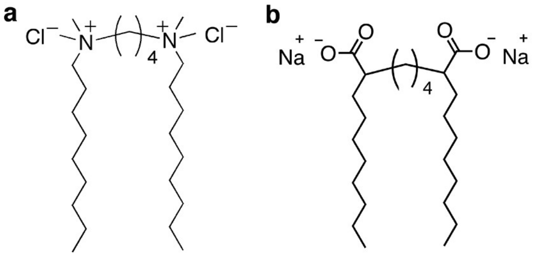

Figure 1. Chemical structures of (*a*) well-studied 4° gemini bis(ammonium) surfactants in which the hydrophobic linker is connected through the cationic headgroups, (*b*) gemini dicarboxylate surfactants, wherein the linker is attached at the α-position relative to the anionic headgroup.

surfactants governs their overall ability to form any LLC phases, especially, their capacity to adopt LLC Q-phases.[22]

In contrast to the relatively narrow temperature versus composition G_I-phase windows observed in bis(phosphonium) and bis(ammonium) surfactants, the gemini dicarboxylate amphiphiles reported by Sorenson *et al*. exhibit substantially larger lyotropic G_I-phase windows that are up to ~ 20 wt% wide between T = 22–100 °C (Figure 1b).[6] Lengthening the hydrophobic linker from butane-1,4-diyl ($–C_4H_8–$) to hexane-1,4-diyl ($–C_6H_{12}–$) in gemini dicarboxylates enlarges the observed lyotropic G_I-phase, while simultaneously destabilizing the L_α phase in favor of other non-constant mean curvature LLC structures. Since lengthening the hydrophobic surfactant tails apparently drives formation of constant mean curvature phases (L_α and H), tuning the relative linker and tail lengths enables subtle manipulation of LLC interfacial curvature to stabilize new phases, including the 3D-hexagonal H_I^{193} network.[5] Finally, recently reported "odd-even" linker length effects drive the expansion of the LLC G_I-phase window to a remarkable width of ~45 wt% dicarboxylate amphiphile at 22 °C.[21] Therefore, gemini dicarboxylate surfactant LLC phase behavior sensitively depends on the lengths of the hydrophobic tails and the hydrophobic linker, as well as the identity of the charge compensating counterion. The significantly wider G_I-phase observed in gemini dicarboxylate amphiphiles as compared to 4° bis(ammonium) and bis(phosphonium) surfactants highlights the notable absence of obvious amphiphile design criteria, which enable rational manipulation of the subtle non-covalent force balance governing their supramolecular self-assembly into LLC networks.[23]

Beyond the obvious chemical difference between their headgroups, careful inspection of the molecular structures of the 4° bis(ammonium) and dicarboxylate gemini amphiphiles reveals differences in the position of the hydrophobic bridge that links the constituent single-tail surfactants (Figure 1). While the hydrophobic linker directly connects the hydrophilic headgroups in the bis(ammonium) surfactants, the linker is necessarily located one carbon away from the headgroups in the dicarboxylates amphiphiles. Recent molecular dynamics (MD) simulations of dicarboxylate gemini surfactants suggest that they adopt unusual, splayed conformations that facilitate G_I formation. These experimental and MD simulations insights spurred us to hypothesize that the position of the hydrophobic linker in a gemini amphiphile relative to the hydrophilic headgroup may generally affect its preferred molecular conformations upon headgroup hydration, thus influencing its lyotropic self-assembly behavior.

Herein, we describe the synthesis and aqueous lyotropic phase behavior of a homologous series of 4° gemini bis(ammonium) dichloride surfactants, in which the position of the hydrophobic linker is systematically varied. Our studies reveal that the position of the linker relative to the amphiphile headgroups sensitively controls the preferred interfacial curvature adopted by the LLC assembly. Within this bis(ammonium) surfactant series, we specifically demonstrate that judicious selection of the linker position renders the aqueous lyotropic G_I-phase accessible over a phase window that is ~12 wt% wide in amphiphile concentration between T = 22-100 C.

Results & Analysis

Based on the above hypothesis regarding the origin of the differences in the LLC phase behaviors of bis(ammonium) and dicarboxylate gemini amphiphiles, we synthesized the series of bis(ammonium) surfactants depicted in Figure 2. We

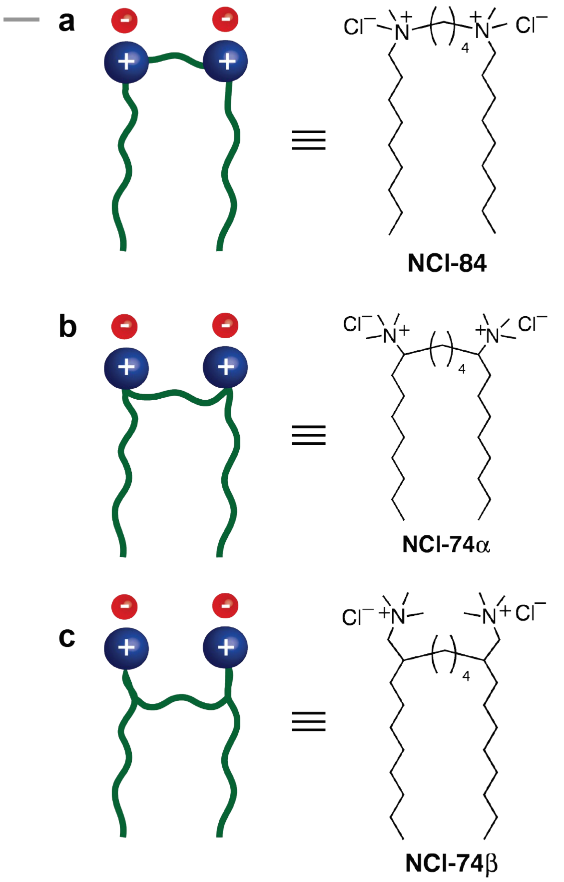

Figure 2. Schematic depictions and chemical structures of homologous of 4° bis(ammonium) gemini surfactants with the linker positioned at: (*a*) the hydrophilic headgroups in **NCl-84**, (*b*) the α-position adjacent to the headgroups in **NCl-74α**, and (*c*) the β-position relative to the headgroup in **NCl-74β**.

Scheme 1. Synthesis of gemini surfactant **NCl-84**.

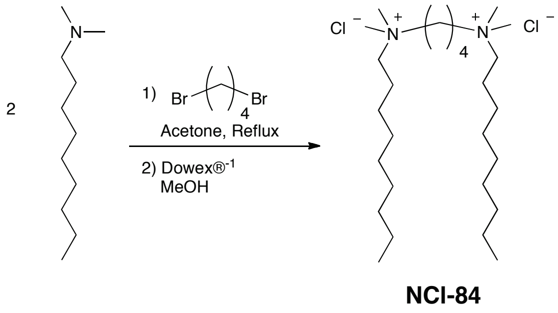

specifically sought to synthesize a homologous series of molecules in which two single-tail 4° ammonium amphiphiles were tethered through a four-carbon linker at the headgroups as in **NCl-84** (Figure 2a), at the α-position adjacent to the headgroups as in **NCl-74α** (Figure 2b), and at the β-position relative to the headgroups as in **NCl-74β** (Figure 2c). In this series, we maintained a constant number of carbon atoms in the hydrophobic portion of the amphiphiles to simplify the comparative analysis of their lyotropic phase behaviors.

We synthesized the gemini surfactant **NCl-84** with the linker positioned at the headgroup through the reaction of two equivalents of commercially available *N,N*-dimethylnonylamine with 1,4-dibromobutane to afford a 4° bis(ammonium) dibromide surfactant, by analogy with a previous report (Scheme 1).[24] Treatment of this synthetic intermediate with Dowex®-1 chloride anion exchange resin furnished the desired **NCl-84** bearing Cl^- counterions. Chloride counterions were chosen to enhance the hydration ability of the surfactants, and thus increase their propensity to form LLC phases in H_2O. (See Supporting Information for detailed experimental procedures.)

Quaternary bis(ammonium) surfactant **NCl-74α**, in which the linker connects the two surfactants at the α-position adjacent to the 4° ammonium headgroups, was synthesized from our previously reported dicarboxylate gemini surfactant docosane-9,14-dicarboxylic acid (**1**)[6] in the three steps shown in Scheme 2. Subjecting **1** to Schmidt reaction conditions by treatment with NaN_3 and concentrated H_2SO_4 in benzene results in the efficient formation of a gemini bis(alkyl isocyanate), which undergoes subsequent alkaline hydrolysis with NaOH(*aq*) to yield the diamine **2**.[25] Exhaustive methylation of **2** with CH_3I, followed by Cl^- ion exchange using the Dowex®-1 resin yields the desired 4° bis(ammonium) surfactant, **NCl-74α**.

Gemini dicarboxylate **1** also serves as a versatile starting material for the synthesis of **NCl-74β** by the route depicted in Scheme 3. We first synthesized diamide **3** by sequential reaction of diacid **4.1** with $SOCl_2$ and $HNMe_2$ in THF at 22 °C. Complete amide reduction of **3** using $LiAlH_4$ furnishes the 3° diamine **4**, which was permethylated with CH_3I to yield the desired 4° bis(ammonium) surfactant scaffold. Iodide ion exchange was again achieved by treatment with Dowex®-1 chloride anion exchange resin to yield **NCl-74β** in 38% overall yield based on **1**.

The LLC phase behaviors of the series of gemini surfactants **NCl-84**, **NCl-74α**, and **NCl-74β** were studied by variable temperature lab source and synchrotron small-angle X-ray scattering (SAXS) between T = 22–100 °C. LLCs were produced by hydration of each of the rigorously dried surfactant salts with carefully measured amounts of H_2O to produce a series of samples with compositions varying in 5 wt% increments. All samples were allowed to rest under quiescent conditions for at least 12 h prior to SAXS analysis, in order to allow relaxation of residual stresses in the samples arising from preparation by high-speed centrifugation. We note that while phase coexistence windows situated between the pure LLC phase windows documented below are anticipated in accordance with Gibbs' phase rule,[21, 26] the 5 wt% composition resolution of our phase maps did not always reveal their presence; only phase coexistence windows that are > 2.5 wt% wide are noted in the following discussion.

Scheme 2. Synthesis of gemini surfactant **NCl-74α**

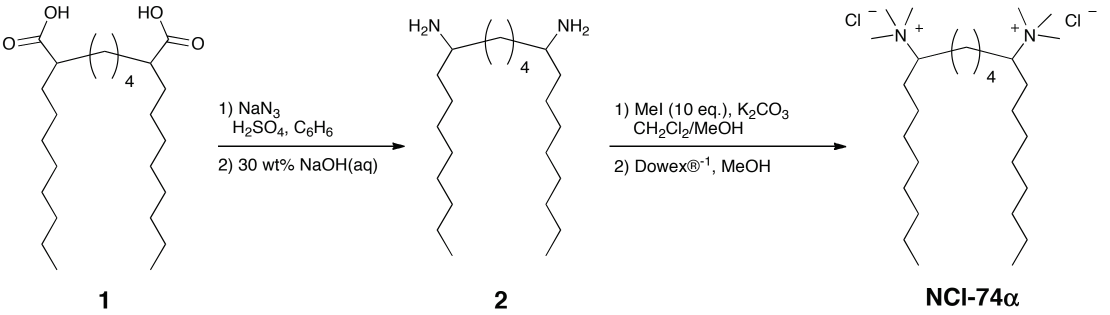

Scheme 3. Synthesis of gemini surfactant **NCl-74β**

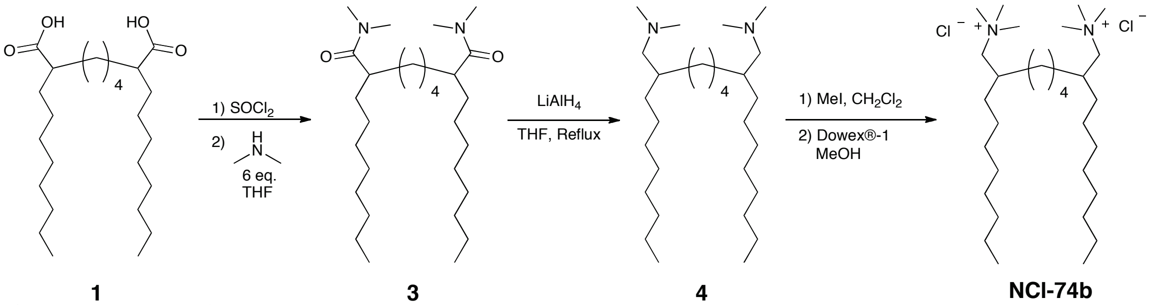

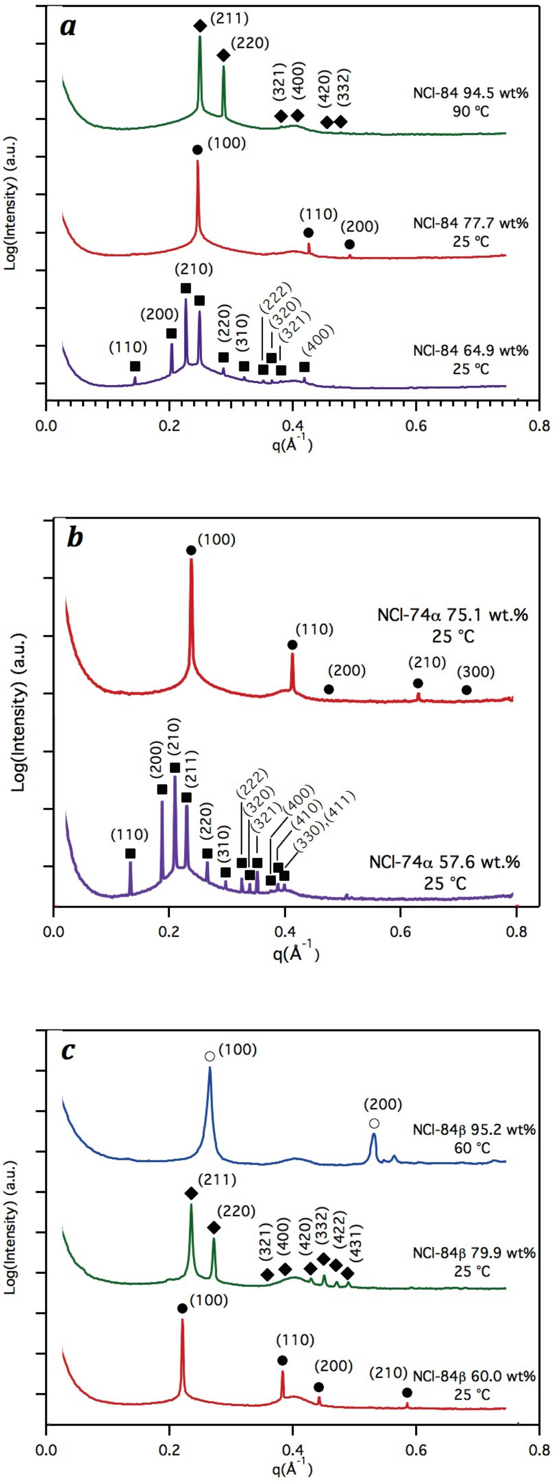

Figure 3. Azimuthally-integrated SAXS patterns for LLCs derived from: (*a*) **NCl-84**, (*b*) **NCl-74α**, and (*c*) **NCl-74β**. Markers on each trace indicate the calculated peak positions for the $Pm\bar{3}n$ (■), H_I (●), G_I (◆) and L_α (○) LLC morphologies. The broad scattering feature at approximately 0.4 Å^{-1} is due to the Kapton® in the synchrotron SAXS sample holder, and the small additional peaks in **NCl-74β** at 95.2 wt% arise from a low degree of surfactant crystallinity at low hydrations.

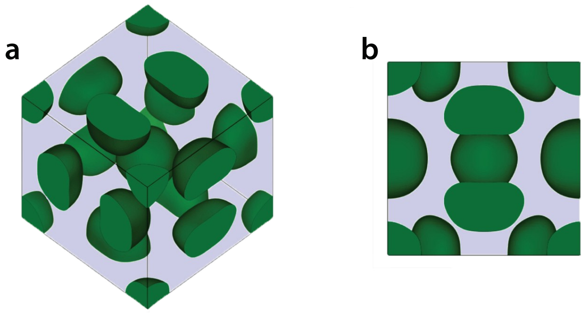

Figure 4. Representation of the micellar arrangement in the $Pm\bar{3}n$ LLC phase adapted from Perroni and Mahanthappa,[32] showing (*a*) the full unit cell, and (*b*) a view of one cell face to highlight the shape of the "platelet" micelles.

NCl-84 forms a series of LLC phases at compositions comprising < 90 wt% surfactant at 25 °C, as the surfactant remains crystalline at lower hydrations (> 90 wt% **NCl-84**) at 25 °C (Figure 3a). We observe a LLC phase between T = 80-100 °C at a composition of 94.5 wt% **NCl-84** that exhibits SAXS maxima at q/q^* = $\sqrt{6}$, $\sqrt{8}$, $\sqrt{14}$, and $\sqrt{16}$ with q^* = 0.1021 Å^{-1}, which is consistent with the formation of a double gyroid (G) phase. In the composition range 85-70 wt% **NCl-84** between T = 25-100 °C, variable-temperature SAXS analyses yield scattering patterns with peaks located at q/q^* = 1, $\sqrt{3}$, and $\sqrt{4}$ with q^* = 0.2460 Å^{-1} that indicate formation of a hexagonally-packed cylinders LLC morphology (H_I). LLC samples comprising 65 wt% **NCl-84** are stiff and optically non-birefringent, suggesting the formation of a LLC with cubic space group symmetry. SAXS patterns associated with this LLC between T = 25-50 °C exhibit scattering peaks at at q/q^* = $\sqrt{2}$, $\sqrt{4}$, $\sqrt{5}$, $\sqrt{6}$, $\sqrt{8}$, $\sqrt{10}$, $\sqrt{12}$, $\sqrt{13}$, $\sqrt{14}$, and $\sqrt{16}$ with q^* = 0.1018 Å^{-1}. This distinctive scattering signature with a somewhat unusual scattered intensity envelope is characteristic of an LLC with $Pm\bar{3}n$ symmetry (space group #223).[3, 27-30] Below 60 wt% **NCl-84**, the surfactant forms disordered normal micellar solutions (L_1). Based on the formation of a L_I phase at high dilutions, we ascertain that these LLCs are Type I ("normal") phases with the water concentration-dependent phase progression: $G_I \rightarrow H_I \rightarrow Pm\bar{3}n \rightarrow L_1$ (micelles).

The groups of Luzzati,[30] Imperor–Clerc,[27] and Warr[28] have previously reported the formation of Type I $Pm\bar{3}n$ LLCs or Frank-Kasper A15 structures, while Perroni and Mahanthappa recently reported the A15 structure as a Type II LLC phase.[29] Percec and co-workers have also described a related structure in thermotropic liquid crystals.[31, 32] This discontinuous cubic LLC structure formed by **NCl-84** is a tetrahedral close packing of quasi-spherical micelles with two different preferred shapes in an AB_3 stoichiometry (Figure 4).[31] One set of spherical micelles are arranged on a body-centered cubic lattice, with one micelle at the center of the unit cell and one micelle located at each of the eight corners. A second set of "platelet" micelles are placed pairwise in each of the six faces of the cube in a manner that renders the unit cell diagonal a $\bar{3}$-axis.

We have summarized the phase behavior of **NCl-84** in the temperature versus amphiphile concentration LLC phase diagram shown in Figure 5a. The observed phase behavior is consistent with that previously reported for other 4° bis(ammonium) gemini surfactants,[22] especially, the wide H_I-phase window and the narrow G_I-phase window that is

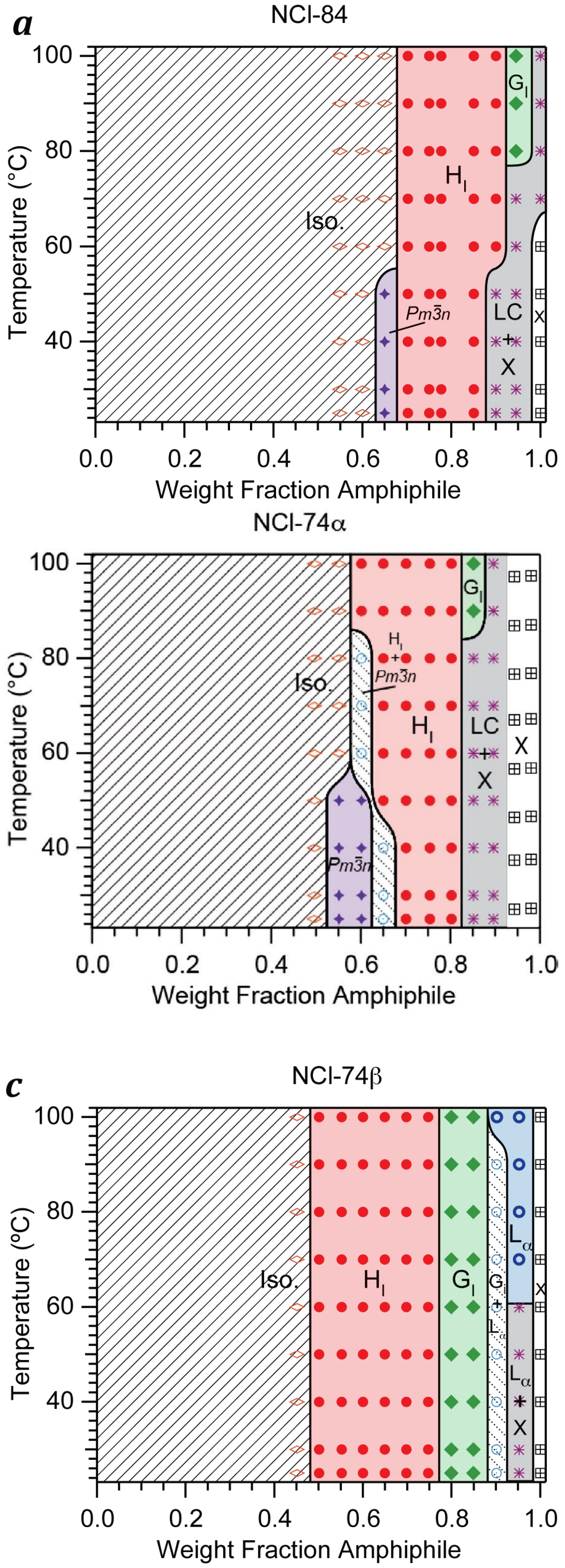

Figure 5. Temperature *vs.* concentration aqueous LLC phase diagrams for (*a*) **NCl-84**, (*b*) **NCl-74α**, and (*c*) **NCl-74β** gemini amphiphiles: Iso. = fluid isotropic phase, *Pm*$\bar{3}$*n* = normal discontinuous cubic micelle (A15) packing, H$_I$ = normal hexagonal, G$_I$ = normal Gyroid, L$_\alpha$ = lamellar, and X = crystalline surfactant.

accessible only at elevated temperatures. Note that the pure L$_\alpha$ LLC phase is absent, even at higher temperatures.

LLCs comprising 55-90 wt% **NCl-74α** over the temperature range *T* = 25-100 °C exhibit a similar phase progression with decreasing surfactant content analogous to **NCl-84**. Two representative azimuthally-integrated synchrotron SAXS patterns for LLCs derived from **NCl-74α** are shown in Figure 3b. Similar to **NCl-84**, **NCl-74α** exhibits a narrow G$_I$ mesophase window at a surfactant concentration of 85 wt% between *T* = 90-100°C with no accessible L$_\alpha$ phase; below 90 °C, only heterogenous mixtures of crystalline surfactant and a poorly defined LLC are observed. In the concentration window between 70-80 wt% **NCl-74α***,* we observe an H$_I$ mesophase. Lowering the surfactant content to 55-60 wt%, **NCl-74α** again results in the formation of stiff solids that exhibit unique SAXS signatures of the discontinuous cubic *Pm*$\bar{3}$*n* micelle packing (*q/q** = √2, √4, √5, √6, √8, √10, √12, √13, √14, √16, √17, and √18 as in Figure 4b). In between the H$_I$ and *Pm*$\bar{3}$*n* pure phase windows, we observe a significant window of two-phase coexistence. Again, **NCl-74α** forms a L$_1$ disordered, normal micellar dispersion when the surfactant concentration drops below 55 wt%. The LLC phase behavior of **NCl-74α** is summarized in the phase diagram in Figure 5b.

Derived from the SAXS analyses presented in Figure 3c, the aqueous LLC phase diagram for **NCl-74β** is given in Figure 5c. Notably, **NCl-74β** forms ordered phases over a somewhat broader amphiphile concentration window spanning 50-95 wt% in H_2O. Disordered micelle solutions (L$_1$) form below 50 wt% **NCl-74β**, evidenced by the absence of any sharp structure factor scattering by SAXS. In contrast to the observed *Pm*$\bar{3}$*n* micellar phase in **NCl-84** and **NCl-74α** at concentrations bordering the composition-dependent LLC lattice ordering transition at high hydrations, LLCs comprising 50-75 wt% **NCl-74β** form a H$_I$ mesophase between 25-100 °C. No *Pm*$\bar{3}$*n* phase is observed in this surfactant system. At 80 and 85 wt% **NCl-74β**, we observed a well-ordered and pure G$_I$ mesophase; however, coexisting G$_I$ and L$_\alpha$ phases are observed at 90 wt% **NCl-74β**. Under the minimal hydration condition of 95.2 wt% at *T* > 60 °C, **NCl-74β** forms a L$_\alpha$ phase evidenced by SAXS maxima at *q/q** = 1 and 2. The apparent thermal insensitivity of the observed LLC phases contrasts the phase behaviors of **NCl-84** and **NCl-74α** and is reminiscent of the aqueous lyotropic behavior gemini dicarboxylate surfactant **NMe$_4$-74** reported previously.[6]

Comparison of the phase diagrams presented in Figure 5 provides insights into the similarities and differences in the LC phase behaviors of these three surfactants. From the onset of crystallization near 85 wt% **NCl-74α** as compared to 90 wt% for **NCl-84** and 95 wt% for **NCl-74β,** we deduce that the headgroup-counterion pair of **NCl-74β** is the most easily hydrated. The wider *Pm*$\bar{3}$*n* LLC composition window and the large region of H$_I$/*Pm*$\bar{3}$*n* coexistence in the **NCl-74α** phase diagram both suggest a propensity for **NCl-74α** to form more highly curved aggregates with non-constant mean curvatures than **NCl-84**. However, **NCl-74β** exhibits the greatest propensity to form non-constant mean curvature LLCs, as revealed by the stabilization of the G$_I$-phase over a LLC composition window spanning 10 wt% in concentration between 25-100 °C.

Discussion

The LLC self-assembly behavior of the homologous 4° bis(ammonium) gemini surfactants may be rationalized using the conceptual framework recently proposed by Mondal *et al.*[33] Their molecular dynamics simulations of gemini dicarboxylate LLC self-assembly revealed that formation of non-constant mean curvature aqueous lyotropic G_I phases is primarily controlled by electrostatic repulsions between the solvated surfactant headgroups, which sensitively depend on the extent of headgroup-counterion dissociation. Solvation of the ionic headgroups triggers counterion-headgroup dissociation, which leads to: (1) unfavorable *intramolecular* Coulombic repulsions between the tethered headgroups that force adoption of the splayed molecular conformation of the surfactant depicted in Figure 6, and (2) unfavorable *intermolecular* Coulombic repulsions between headgroups of adjacent surfactant molecules. The observed supramolecular LLC morphology reflects the balance of these repulsions against the van der Waals attractions between the tails and the "hydrophobic effect" that drives their sequestration. Mondal *et al.* reason that the tight surfactant packing in a L_α-phase is electrostatically destabilized by Coulombic repulsions between hydrated headgroup-counterion pairs. At intermediate hydration levels, the diminished stability of the L_α phase drives G_I phase formation due to the highly anisotropic molecular conformation adopted by the surfactant. Highly curved, gemini dicarboxylate H_I-phases form only when the counterion is so highly dissociated from the headgroup that the twin hydrophobic tails are forced to "tuck back" together. Therefore, non-constant mean curvature gyroid phases form when headgroup-counterion ion pair dissociation is most sensitive to subtle differences in hydration *and* when the gemini surfactant can adopt a splayed conformation.

Comparison of the LLC phase diagrams in Figure 5 also highlights the fact that the linker position in 4° bis(ammonium) gemini surfactants controls the maximum hydration capacity of their headgroup-counterion pairs. At the concentration where one observes a transition from a structured LLC to a disordered micellar solution (L_1 phase), the surfactant headgroup-counterion pairs are fully solvated and the excess water triggers lattice disordering. With the onset of LLC ordering at 65 wt% for **NCl-84** as compared to 55 wt% for **NCl-74α** and 50 wt% for **NCl-74β**, we conclude the surfactant hydration capacity increases along the series:

NCl-84 < **NCl-74α** < **NCl-74β**

We rationalize this trend by noting that **NCl-84** has the most sterically encumbered 4° ammonium headgroups in this series (Figure 1a). This steric bulk drives the greatest degree of counterion-headgroup ion pair dissociation, which facilitates the complete hydration of the **NCl-84** headgroups.[34, 35] On the other hand, **NCl-74β** has the most sterically unencumbered headgroup (Figure 1c) and thus the most tightly associated counterion-headgroup ion pairs relative to **NCl-74α** and **NCl-84**. Consequently, **NCl-74β** requires the largest number of hydrating water molecules for headgroup-counterion dissociation, rendering it the most sensitive to subtle hydration state differences.

The LLC phases formed by **NCl-84**, **NCl-74α**, and **NCl-74β** reflect the extent of counterion-headgroup dissociation therein. Romsted and co-workers experimentally noted that increasing headgroup-counterion dissociation drives the formation of higher curvature micellar aggregates in dilute solutions of 4° ammonium single-tail and gemini surfactants.[34, 36, 37] On this basis, the preference for both **NCl-84** and **NCl-74α** to form a micellar $Pm\bar{3}n$ LLC phase with highly curved interfaces mirrors the deduced higher degrees of counterion-headgroup dissociation in these hydrated surfactants (*vide supra*). The aforementioned experiments by Romsted and co-workers also suggest that the occurrence of an L_α-phase only in **NCl-74β** implies that counterion-headgroup ion pairing is tightest in this surfactant. This ion pairing behaviour allows for dehydration of the hydrophobic/hydrophilic interface to form a L_α phase.

The listing of the observed LLC phase as a function of the headgroup hydration number λ (= mol H_2O/s mol gemini surfactant headgroups derived from mass balance, including any H_2O associated with the nominally dry surfactant; see Supporting Information for elemental analysis details) for **NCl-84**, **NCl-74α**, and **NCl-74β** given in Table 1 quantitatively supports the deduced extent of counterion-headgroup dissociation. When $\lambda \approx 15$, the preferred interfacial curvature of the LLC flattens from the quasi-spherical micelles of $Pm\bar{3}n$ in **NCl-84** to the cylindrical micelles of the H_I phase of **NCl-74β** upon moving the linker farther away from the hydrophilic headgroup, consistent with a greater degree of counterion-headgroup association. A similar transition from H_I to G_I is observed at $\lambda \approx 7$, which follows a similar trend in decreasing interfacial curvature (or increased counterion-headgroup association) as the hydrophobic linker is moved farther from the cationic ammonium headgroups. Note that this comparative analysis of the morphology adopted at a given headgroup hydration number is only valid for surfactants that have approximately the same hydrophobic volume and headgroup chemistry, as is the case in the series **NCl-84**, **NCl-74α**, and **NCl-74β** presented here.

While the extent of counterion-headgroup dissociation accounts for the relative stabilities of the micellar and lamellar phases of **NCl-84**, **NCl-74α**, and **NCl-74β**, the molecular conformation of the gemini surfactant plays an integral role

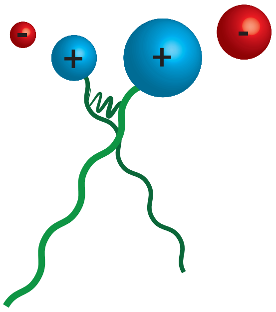

Figure 6. Schematic depiction of the conformation adopted by a hydrated gemini surfactant linked through a position adjacent to the hydrophilic headgroup, in which the hydrophobic tails splay in order to mitigate intramolecular Coulombic repulsions between the headgroups.

Table 1. Linker position dependence of LLC morphology at comparable surfactant hydration numbers (λ)

Sample	λ^a	wt%	Phase
NCl-84	14.0	65.0	$Pm\bar{3}n$
	7.8	77.0	H_I
NCl-74α	14.9	65.0	$Pm\bar{3}n$ + H_I
	6.8	80.2	H_I
NCl-74β	15.8	64.9	H_I
	7.3	79.9	G_I

[a] λ = mol H_2O/2 mol gemini surfactant headgroups derived from mass balance, including any H_2O associated with the nominally dry surfactant; see Supporting Information for elemental analysis details

in the formation of the non-constant mean curvature G_I LLC. Upon counterion dissociation from the cationic headgroup of **NCl-74β**, we speculate that this surfactant adopts a conformation in which the tails splay apart as in Figure 6. This splayed conformation mitigates intramolecular Coulombic repulsions, by increasing the intramolecular distance between cationic headgroups. Since anisotropic surfactant inclusions favor non-constant mean curvature LLC phase selection,[38] this conformation enables formation of a G_I-phase over a 12 wt% wide composition window from 25–100 °C. The preference for a splayed tail conformation also prevents the higher curvature $Pm\bar{3}n$ phase from forming, as this morphology requires the surfactant tails to "tuck back" together to form a quasi-spherical micelle. At the other extreme, **NCl-84** cannot adopt any splayed conformations that mitigate intermolecular headgroup repulsions, since the linker is directly attached to the cationic headgroups (see Figure 1a). Consequently, **NCl-84** forms only high curvature H_I and $Pm\bar{3}n$ LLCs. While an intermediate level of twin tail splay in **NCl-74α** is expected, we surmise the high degree of counterion-headgroup dissociation drives the formation of the high curvature LLC phases. Thus, the ability of the surfactants to adopt non-constant mean curvature LLC morphologies increases in the order:

NCl-84 < **NCl-74α** < **NCl-74β**

The changes in preferred LLC interfacial curvature upon moving the linker down the alkyl tail of a gemini surfactant are reminiscent of the effects of changing the counterion on gemini dicarboxylate LLC phase behavior. Strong interactions between Na^+ cations and the carboxylate headgroups manifest in the wide G_I and L_α phase windows with low interfacial curvatures. Similarly, strong counterion-headgroup interactions in **NCl-74β** result in the analogous stabilization of LLCs with lower degrees of interfacial curvature. Replacing the Na^+ with a highly dissociated NMe_4^+ counterion in the gemini dicarboxylates enforces formation of highly curved H_I phases over wide composition ranges, and the G_I LLC appears only at very low hydration numbers. This observation parallels the formation of high curvature H_I LLCs from **NCl-84**. Thus, the linker position in ammonium gemini surfactants controls the extent of ion pairing between the headgroup and the counterion and its sensitivity to the surfactant hydration state. These results suggest that judicious positioning of the linker in any gemini surfactant may enable manipulation of its allowed molecular conformations upon hydration, and its consequent intermolecular packings that direct LLC phase selection.

Direct comparison of the lyotropic phase behaviors of the previously reported gemini dicarboxylate surfactants and those considered herein reveals that the width of the lyotropic gyroid phase window for the bis(ammonium) surfactant **NCl-74β** is much narrower (20 wt % versus ~12 wt%, respectively). We ascribe this phase behaviour variation to differences in headgroup chemistries. We note that a carboxylate is a monoanionic headgroup in which the negative charge is delocalized over two oxygen atoms, whereas the quaternary ammonium headgroup is monocationic with positive charge delocalized over four carbon atoms. Thus, the charge in the ammonium surfactant is significantly more delocalized. We speculate that this charge delocalization in the ammonium headgroups reduces the electrostatically-driven propensity for tail splay, which destabilizes the lyotropic G_I phase window. On this basis, we hypothesize that the degree of charge (de)localization in the headgroups of a gemini surfactant will necessarily impact the extent of tail splay and the consequent lyotropic network phase stability.

Conclusion

We have synthesized and characterized the LLC behavior of a series of homologous 4° ammonium gemini surfactants, in which the attachment position of the linker was systematically varied relative to the hydrophilic headgroup. The linker position dramatically influences the LLC phase behavior, by modulating the extent to which the counterion and ammonium headgroup dissociate and the sensitivity of this dissociation equilibrium to hydration. When the linker is attached directly to the headgroup, the headgroup-counterion pair more fully dissociates and is easily hydrated to form high curvature LLC morphologies. Moving the linker down the alkyl tails away from the ionic headgroups reduces the steric bulk around the ammonium functionality, thereby allowing stronger headgroup-counterion association. These increased correlations coupled with their increased sensitivity to hydration opens LLC phase windows with lower interfacial curvatures, including the useful gyroid (G_I) network phase. These results demonstrate that the ability to dictate the LLC morphologies adopted by gemini amphiphiles critically hinges on finely controlling both counterion-headgroup correlations and surfactant conformations at modest hydration numbers.

Acknowledgements

We acknowledge financial support for this work from the U. S. National Science Foundation (CHE-1152347) and a 3M Science and Technology Graduate Fellowship to G.P.S.. This work also utilized central facilities at the University of Wisconsin–Madison funded in part by NSF grants for mass spectrometry (CHE-9974839), NMR spectroscopy (CHE-1048642) and supplementary gift funds from Paul J. Bender, the UW-Madison NSEC (DMR-0425880 and DMR-0832760), and the CEMRI (DMR-0520527 and DMR-1121288). Synchrotron SAXS studies were conducted at Sector 12 of the Advanced Photon Source at Argonne National Laboratory, which is supported by the U.S. DOE under Contract #DE-AC02-06CH11357.

Notes and References

1. J. M. Seddon, R. H. Templer, R. Lipowsky and E. Sackmann, in *Handbook of Biological Physics*, North Holland (Elsevier), New York, 1995, vol. Volume 1, Part 1, pp. 97-160.
2. C. E. Fairhurst, S. Fuller, J. Gray, M. C. Holmes and G. J. T. Tiddy, in *Handbook of Liquid Crystals*, eds. D. Demus, J. W. Goodby, G. W. Gray, H. W. Spiess and V. Vill, Wiley-VCH, Weinheim, 1998, vol. 3, pp. 341-392.
3. S. T. Hyde, in *Handbook of Applied Surface and Colloid Chemistry*, ed. K. Holmberg, John Wiley & Sons, Inc., New York, 2001, vol. 1, pp. 299-332.
4. T. Kato, N. Mizoshita and K. Kishimoto, *Angew. Chem., Int. Ed.*, 2006, **45**, 38-68.
5. G. P. Sorenson, A. K. Schmitt and M. K. Mahanthappa, *Soft Matter*, 2014, **10**, 8229-8235.
6. G. P. Sorenson, K. L. Coppage and M. K. Mahanthappa, *J. Amer. Chem. Soc.*, 2011, **133**, 14928-14931.
7. D. L. Gin, J. E. Bara, R. D. Noble and B. J. Elliott, *Macromol. Rapid Commun.*, 2008, **29**, 367-389.
8. E. S. Hatakeyama, B. R. Wiesenauer, C. J. Gabriel, R. D. Noble and D. L. Gin, *Chem. Mater.*, 2010, **22**, 4525-4527.
9. M. Caffrey, D. Li and A. Dukkipati, *Biochemistry*, 2012, **51**, 6266-6288.
10. V. Cherezov, *Curr. Opin. Struct. Biol.*, 2011, **21**, 559-566.
11. C. Leal, N. F. Bouxsein, K. K. Ewert and C. R. Safinya, *J. Amer. Chem. Soc.*, 2010, **132**, 16841-16847.
12. J. Zhang, Y. Pei, H. Zhang, L. Wang, L. Arrington, Y. Zhang, A. Glass and A. M. Leone, *Mol. Pharmaceut.*, 2013, **10**, 397-405.
13. C. Xiao, N. Fujita, K. Miyasaka, Y. Sakamoto and O. Terasaki, *Nature*, 2012, **487**, 349-353.
14. K. Czechura and A. Sayari, *Chem. Mater.*, 2006, **18**, 4147-4150.
15. L. Han and S. Che, *Chem. Soc. rev.*, 2013, **42**, 3740-3752.
16. C. B. Gao, H. B. Qiu, W. Zeng, Y. Sakamoto, O. Terasaki, K. Sakamoto, Q. Chen and S. A. Che, *Chem Mater*, 2006, **18**, 3904-3914.
17. C. B. Gao, Y. Sakamoto, O. Terasaki and S. A. Che, *Chem-Eur J*, 2008, **14**, 11423-11428.
18. M. In and R. Zana, *J. Disper. Sci. Technol.*, 2007, **28**, 143-154.
19. H. Kunieda, N. Masuda and K. Tsubone, *Langmuir*, 2000, **16**, 6438-6444.
20. B. A. Pindzola, J. Jin and D. L. Gin, *J. Am. Chem. Soc.*, 2003, **125**, 2940-2949.
21. D. V. Perroni, C. M. Baez-Cotto, G. P. Sorenson and M. K. Mahanthappa, *J. Phys. Chem. Lett.*, 2015, **6**, 993-998.
22. E. Alami, H. Levy, R. Zana and A. Skoulios, *Langmuir*, 1993, **9**, 940-944.
23. S. Svenson, *J. Disper Sci. Tech.*, 2004, **25**, 101-118.
24. L. Mivehi, R. Bordes and K. Holmberg, *Langmuir*, 2011, **27**, 7549-7557.
25. D. M. Hall, S. Mahboob and E. E. Turner, *J. Chem. Soc. (Resumed)*, 1950, 1842-1845.
26. K. K. Karukstis, W. C. Duim, G. R. Van Hecke and N. Hara, *J. Phys. Chem. B*, 2012, **116**, 3816-3822.
27. M. Clerc, *J. Phys. II France*, 1996, **6**, 961-968.
28. C. K. Liu and G. G. Warr, *Soft Matter*, 2014, **10**, 83-87.
29. D. V. Perroni and M. K. Mahanthappa, *Soft Matter*, 2013, **9**, 7919-7922.
30. R. Vargas, P. Mariani, A. Gulik and V. Luzzati, *J. Mol. Biol.*, 1992, **225**, 137-145.
31. V. Percec, M. Peterca, Y. Tsuda, B. M. Rosen, S. Uchida, M. R. Imam, G. Ungar and P. A. Heiney, *Chem–Eur. J.*, 2009, **15**, 8994-9004.
32. S. D. Hudson, H. T. Jung, P. Kewsuwan, V. Percec and W. D. Cho, *Liq. Cryst.*, 1999, **26**, 1493-1499.
33. J. Mondal, M. Mahanthappa and A. Yethiraj, *J. Phys. Chem. B*, 2013, **117**, 4254-4262.
34. V. Soldi, J. Keiper, L. S. Romsted, I. M. Cuccovia and H. Chaimovich, *Langmuir*, 2000, **16**, 59-71.
35. M. Benrraou, B. L. Bales and R. Zana, *J. Phys. Chem. B*, 2003, **107**, 13432-13440.
36. Y. Geng, L. S. Romsted, S. Froehner, D. Zanette, L. J. Magid, I. M. Cuccovia and H. Chaimovich, *Langmuir*, 2005, **21**, 562-568.
37. Y. Geng, L. S. Romsted and F. Menger, *J. Amer. Chem. Soc.*, 2006, **128**, 492-501.
38. J. B. Fournier, *Phys. Rev. Lett.*, 1996, **76**, 4436-4439.

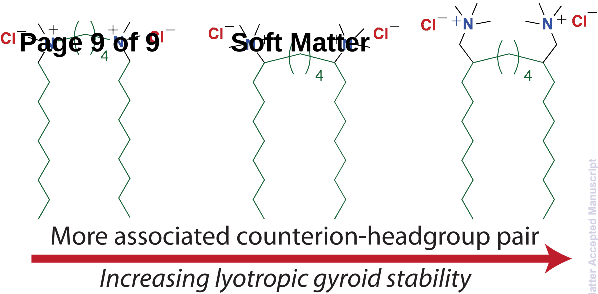

The aqueous lyotropic phase behaviors of homologous gemini bis(ammonium) surfactants demonstrate that the linker location impacts the gyroid phase stability.